

AD-A106 755 NAVAL OCEANOGRAPHIC OFFICE NSTL STATION MS F/G 8/3
DIGITAL FILTERING OF TIROS-N MID-INFRARED SATELLITE DATA. (U)
AUG 81 R E COULTER, C W HORTON

UNCLASSIFIED NOO-TR-269

SBIE-AD-E001 181

NL

1 OF 1
400 A
100 C
1000 D
10000 E



END
PRINTED
11-81
DTIC

AD A106755

TECHNICAL REPORT

AD-600 1181

TR-269

LEVEL III ①

**DIGITAL FILTERING OF TIROS-N
MID-INFRARED SATELLITE DATA**

ROBERT E. COULTER and CHARLES W. HORTON

DTIC
ELECTE
S NOV 05 1981
D

AUGUST 1981

Approved for public release; distribution unlimited

FILE COPY

PREPARED BY
**COMMANDING OFFICER,
NAVAL OCEANOGRAPHIC OFFICE
NSTL STATION, BAY ST. LOUIS, MS 39432**

PREPARED FOR
**COMMANDER
NAVAL OCEANOGRAPHY COMMAND
NSTL STATION, BAY ST. LOUIS, MS 39432**

811105039



FOREWORD

Two years of TIROS-N satellite data are available for analysis toward the development and testing of algorithms to classify and enhance ocean fronts in the imagery. Unfortunately, the mid-infrared data, which should yield good nighttime sea surface temperatures, are contaminated by a considerable amount of multi-band noise.

The procedure outlined in this report will sufficiently reduce the noise to accomplish the above tasks.



C. H. BASSETT
Captain, USN
Commanding Officer

UNCLASSIFIED

SECURITY CLASSIFICATION OF THIS PAGE (When Data Entered)

| REPORT DOCUMENTATION PAGE | | READ INSTRUCTIONS BEFORE COMPLETING FORM |
|--|---|---|
| 1. REPORT NUMBER TR-269 | 2. GOVT ACCESSION NO. AD-A106755 | 3. RECIPIENT'S CATALOG NUMBER |
| 4. TITLE (and Subtitle) DIGITAL FILTERING OF TIROS-N MID-INFRARED SATELLITE DATA | 5. TYPE OF REPORT & PERIOD COVERED | |
| 7. AUTHOR(s) Robert E. Coulter Charles W. Horton | 8. PERFORMING ORG. REPORT NUMBER | |
| 9. PERFORMING ORGANIZATION NAME AND ADDRESS Naval Oceanographic Office (9100) NSTL Station Bay St. Louis, MS 39522 | 10. PROGRAM ELEMENT, PROJECT, TASK AREA & WORK UNIT NUMBERS | |
| 11. CONTROLLING OFFICE NAME AND ADDRESS | 12. REPORT DATE AUGUST 1981 | |
| | 13. NUMBER OF PAGES 22 | |
| 14. MONITORING AGENCY NAME & ADDRESS (if different from Controlling Office) | 15. SECURITY CLASS. (of this report) UNCLASSIFIED | |
| | 15a. DECLASSIFICATION/DOWNGRADING SCHEDULE | |
| 16. DISTRIBUTION STATEMENT (of this Report) Approved for public release; distribution unlimited. | | |
| 17. DISTRIBUTION STATEMENT (of the abstract entered in Block 20, if different from Report) | | |
| 18. SUPPLEMENTARY NOTES | | |
| 19. KEY WORDS (Continue on reverse side if necessary and identify by block number) Gulf Stream TIROS-N Digital filters Spectrum analysis Data processing Infrared detection Noise Sea surface effects detection Bandpass filters | | |
| 20. ABSTRACT (Continue on reverse side if necessary and identify by block number) Considerable multiband noise, present in the mid-infrared band of TIROS-N images, obscures the location of oceanic fronts. A filtering scheme is described that, upon application to an image containing the Gulf Stream, reduced the noise to an extent where the surface front was clearly visible. | | |

ACKNOWLEDGEMENTS

The authors would like to thank Mr. J. R. Clark of the Naval Ocean Research and Development Activity (NORDA) for his assistance in the operation of the Interactive Digital Satellite Image Processing System which produced the images shown in this document. We also wish to thank Mr. A. G. Voorheis who prepared the figures for publication and Mrs. L. A. Stanley who provided secretarial assistance.

CONTENTS

| | | <u>Page</u> |
|------|--------------|-------------|
| I. | INTRODUCTION | 1 |
| II. | PROCEDURE | 1 |
| III. | CONCLUSION | 4 |
| | REFERENCES | 5 |

FIGURES

| | | |
|------------|---|----|
| Figure 1. | Initial Image: TIROS-N Mid-IR Imagery for March 15, 1979 | 6 |
| Figure 2. | Initial Image After a Linear Intensity Mapping of the Form $Y=AX+B$ where X is the Input Grey Level and Y is the Output Value | 7 |
| Figure 3. | Grey Level Profile Across the Center of the Initial Image from Left to Right | 8 |
| Figure 4. | Natural Log of the FFT'd Image Before Filtering | 9 |
| Figure 5. | Profile of the Transformed, Unfiltered Image Along the Vertical Axis at 0 cycles/pixel on the Horizontal Axis | 10 |
| Figure 6. | Profile of the Transformed, Unfiltered Image Along the Horizontal Axis at -.5 cycles/pixel on the Vertical Axis | 11 |
| Figure 7. | Top View of the Inverse, Gaussian Filter: FILTER 1 | 12 |
| Figure 8. | Profile of the Inverse, Gaussian Filter: FILTER 1 | 13 |
| Figure 9. | IFT'd Image after Applying FILTER 1 | 14 |
| Figure 10. | Profile of Grey Levels Across the Center of the Image in Fig. 9 | 15 |
| Figure 11. | Profile of the Low-pass Gaussian Filter: FILTER 2 | 16 |
| Figure 12. | IFT'd Image after Applying FILTER 2 | 17 |
| Figure 13. | Profile of Grey Levels Across the Center of the Image in Fig. 12. | 18 |
| Figure 14. | Convolved Image | 19 |
| Figure 15. | Profile of Grey Levels Across the Center of the Image in Fig. 14 | 20 |

TABLE

| | | |
|----------|---------------------------------|---|
| Table 1. | Gaussian Filter Characteristics | 3 |
|----------|---------------------------------|---|

| | |
|--------------------|-------------------------|
| Accession For | |
| NTIS GRA&I | |
| DTIC TAB | |
| Unannounced | |
| Justification | |
| By | |
| Distribution/ | |
| Availability Codes | |
| Dist | Avail and/or Special |
| A | |

I. INTRODUCTION

The TIROS-N satellite, put into service in 1978, was the initial operational system of a series of third generation, polar-orbiting, environmental satellites. Of interest to oceanographers was the capability of computing sea surface temperature from the mid-infrared (3.55 - 3.93 μm) and the far-infrared (10.5 - 11.5 μm) channels and of detecting certain surface features associated with water masses and coastal processes from all four available channels.

Of specific interest to the Navy was and still is the detection of fronts (boundaries between water masses) like the Gulf Stream. With two infrared channels for obtaining surface temperature, the TIROS-N data seemed most appropriate for developing and testing an automated frontal detection system for fleet applications.

One major shortcoming of this satellite was the considerable noise present in the mid-infrared channel due to a malfunction in the satellite's power system. The purpose of this document is to describe a filtering scheme to eliminate or at least to sufficiently reduce the noise to allow for any enhancement of the image required to accurately locate the fronts.

While the demise of this satellite in November 1980 ends the utility of this scheme for real-time analysis (assuming the defect is nonrepeatable), there are some practical applications of archived data for the detection of fronts. For instance, the testing and development of algorithms for the classification and/or enhancement of oceanic features and, specifically, their reliability when applied to different locations and to images with varying amounts and types of cloud cover are examples.

II. PROCEDURE

The data processing was performed on the Navy's Interactive Digital Satellite Image Processing System (IDSIPS) described by Pressman and Holyer (1978). Existing software described by the Stanford Technology Corp. (1978) was adequate for the analysis.

The first set of data consisted of a 512-by-512 pixel (picture element) image of the western North Atlantic containing the Gulf Stream (fig. 1). Applying a linear intensity enhancement to the image provides no apparent benefit towards interpretation and, in fact, degrades edge detail as shown in figure 2. A pseudo-color enhancement with 16 colors (not shown) assigned to the 256 grey levels of the image accentuates the noise to a degree where the edges are almost undetectable.

Figure 3 is a cross-section or profile from left to right, centered in the image. The grey level scale appears on the ordinate.

The frequencies where the noise occurs were located by examination of figure 4 which is the natural logarithm of the Fast Fourier Transformed (FFT'd) image. Normally, a finite data set is tapered at the ends to prevent distortion in the spectrum due to the discontinuity in the replicated data. However, some experimentation indicated that the 512-by-512 data set was large enough to approximate an infinite set of data and the tapering was excluded from the scheme. Note that only half of the \log_e FFT is displayed since the missing half is symmetric and, therefore, redundant.

The transformed image exhibits a very narrow band of low frequency noise located at .015 cycles/pixel in the horizontal and uniform in the vertical and a much broader band of high frequency noise. Figure 5 is a profile of the \log_e FFT along the vertical axis at zero cycles/pixel on the horizontal axis. Figure 6 is a profile crossing the same image at the top. In this figure, the low frequency noise is barely discernible while the wider band of high frequency noise is clearly evident at the right end of the profile.

Cleaning up the image was accomplished by applying two Gaussian-shaped filters to the two bands of noise described above. The characteristics of the filters designated as FILTER 1 and FILTER 2 are outlined in table 1. Filtering by the more sophisticated local-statistics method described by Lee (1980) and Willman (1980) was rejected because it appeared to be applicable only to high frequency noise.

The low frequency noise was attacked first with FILTER 1 applied to the image in the transform domain. Figure 7 is a top view of the filter and shows its narrow, elliptical shape. A complementary view across the center of the filter is given in figure 8 which demonstrates its inverse character.

After taking the Inverse Fourier Transform (IFT) of the filtered image, the resulting image was enhanced in the same fashion as the initial image and is displayed in figure 9 along with a profile of grey values (fig. 10) at approximately the same location as the profile in figure 3. The IFT'd image without enhancement (not shown) appeared to be clear of all noise, but figures 9 and 10 indicate the presence of the high frequency noise. Note that the wave-like pattern, most obvious above the cloud cover in the lower right corner of figures 1 and 2, is missing in figure 9 proving the effectiveness of the scheme so far.

Applying FILTER 2, described in table 1 and shown in figure 11, reduced the apparent high frequency noise which is difficult to detect in the enhanced image in figure 12. For comparison, the profile in figure 13 crosses the image at the same location as the profiles in figures 3 and 10. The demarcation between land and water, different water masses (indicated by FRONT), and water and clouds (at the extreme right side) is now obvious.

Table 1. GAUSSIAN FILTER CHARACTERISTICS

| <u>Parameter Description *</u> | <u>FILTER 1</u> | <u>FILTER 2</u> |
|--|------------------------------|--------------------------|
| Gain of filter at zero frequency | 0. | 1. |
| Gain of filter at Nyquist frequency | 1. | 0. |
| Frequency along major axis of filter's elliptical contours at which filter attains $\frac{1}{2}$ its maximum power | .004 cycles/pixel | .20 cycles/pixel |
| Frequency along minor axis of filter's elliptical contours at which filter attains $\frac{1}{2}$ its maximum power | .495 cycles/pixel | .30 cycles/pixel |
| Horizontal (sample) coordinate/frequency of filter center in transform domain | 10 samples/.015 cycles/pixel | 0 samples/0 cycles/pixel |
| Vertical (line) coordinate/frequency of filter center in transform domain | 257 lines/.0 cycles/pixel | 257 lines/0 cycles/pixel |
| Angle relative to horizontal direction of filter orientation in transform domain | 0 degrees | 0 degrees |

* Based on a frequency scale from -0.5 cycles/pixel to +0.5 cycles/pixel.

An attempt to remove the high frequency noise by convolving the image (in the spatial domain) with a 3-by-3 pixel kernal with all elements in the kernal weighted equally was less successful. While the convolved image in figure 14 differs only slightly from the twice-filtered image, the profile of the convolved image (fig. 15) is less demonstrative in delineating features.

III. CONCLUSION

A scheme for noise removal in the 3.55 - 3.93 μm infrared channel of the TIROS-N satellite is proven to be effective.

Low frequency noise is removed with a narrow, inverse Gaussian filter. High frequency noise is removed by either a low-pass Gaussian filter or by convolving the image in the spatial domain. The latter technique is less desirable since edges are smoothed over somewhat and some high frequency noise is still present to clutter the fine detail.

This scheme was applied to another noisy image with similar results. Therefore, the process is nonunique.

REFERENCES

Lee, J.-S., Refined filtering of image noise using local statistics, NRL Report 8374, 12, Naval Research Laboratory, Washington, DC, 1980.

Pressman, A. E. and R. J. Holyer, Interactive Digital Satellite Image Processing System for oceanographic applications, NORDA Technical Note 23, 13, Naval Ocean Research and Development Activity, NSTL Station, MS, 1978.

Willman, W. W., A method for specifying the noise suppression-resolution tradeoff in digital image filtering with local statistics, NRL Report 8447, 16, Naval Research Laboratory, Washington, DC, 1980.

Stanford Technology Corporation, System 101/A software documentation manual, Sunnyvale, CA, 1978.

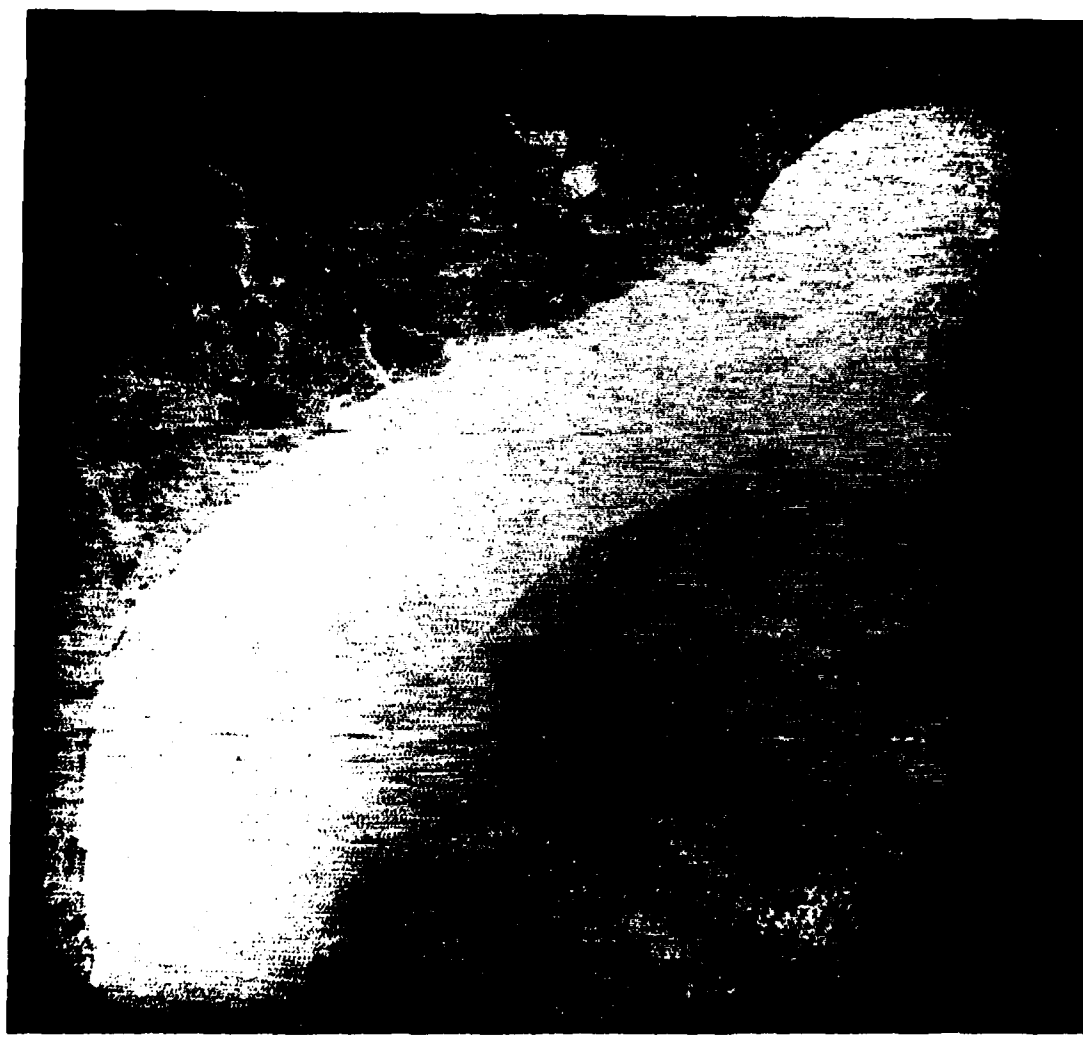


Figure 6. Initial Images - RGB/IR and IR Imagery. 15 March 1993.

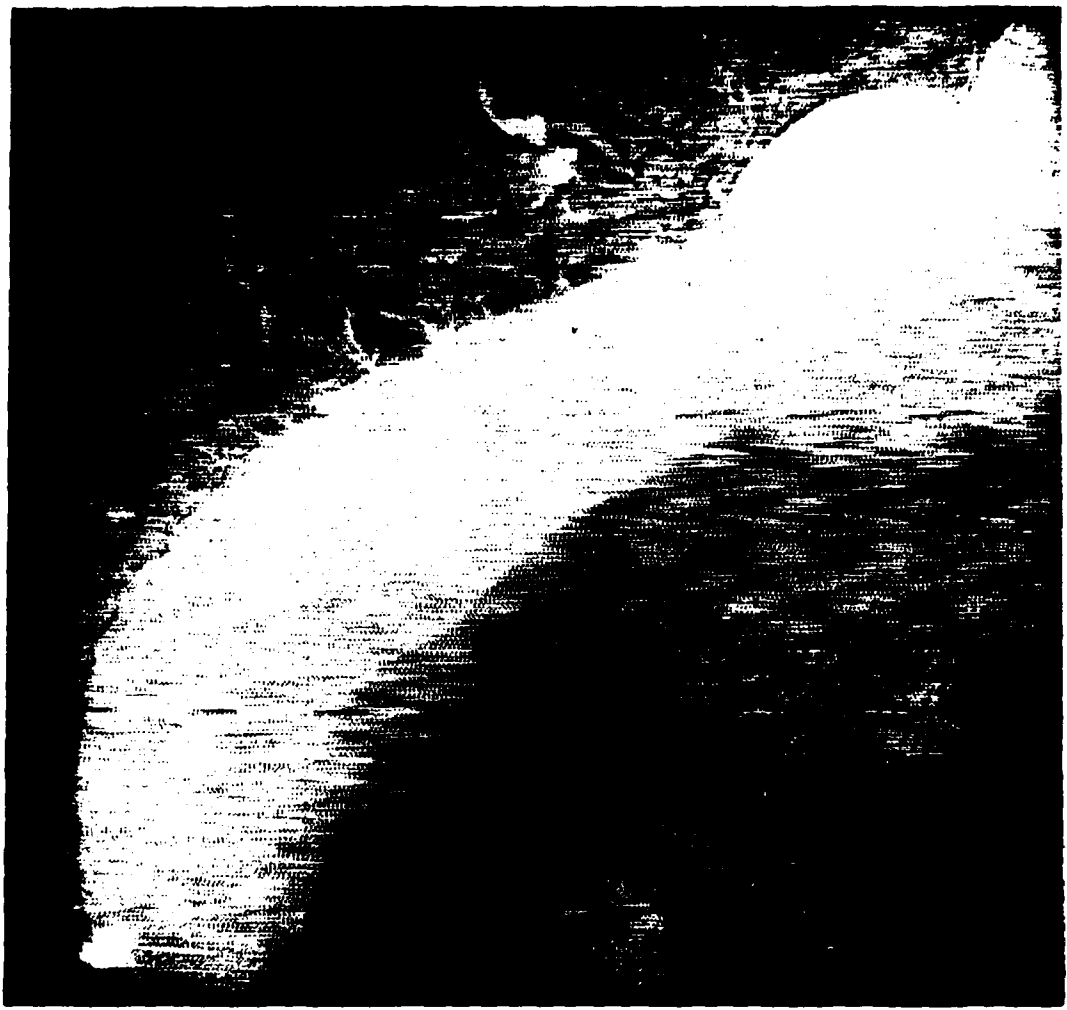


Figure 1. Image after a linear interpolation of 100% of the top 5 AX channels. X is the input image and Y is the output image.

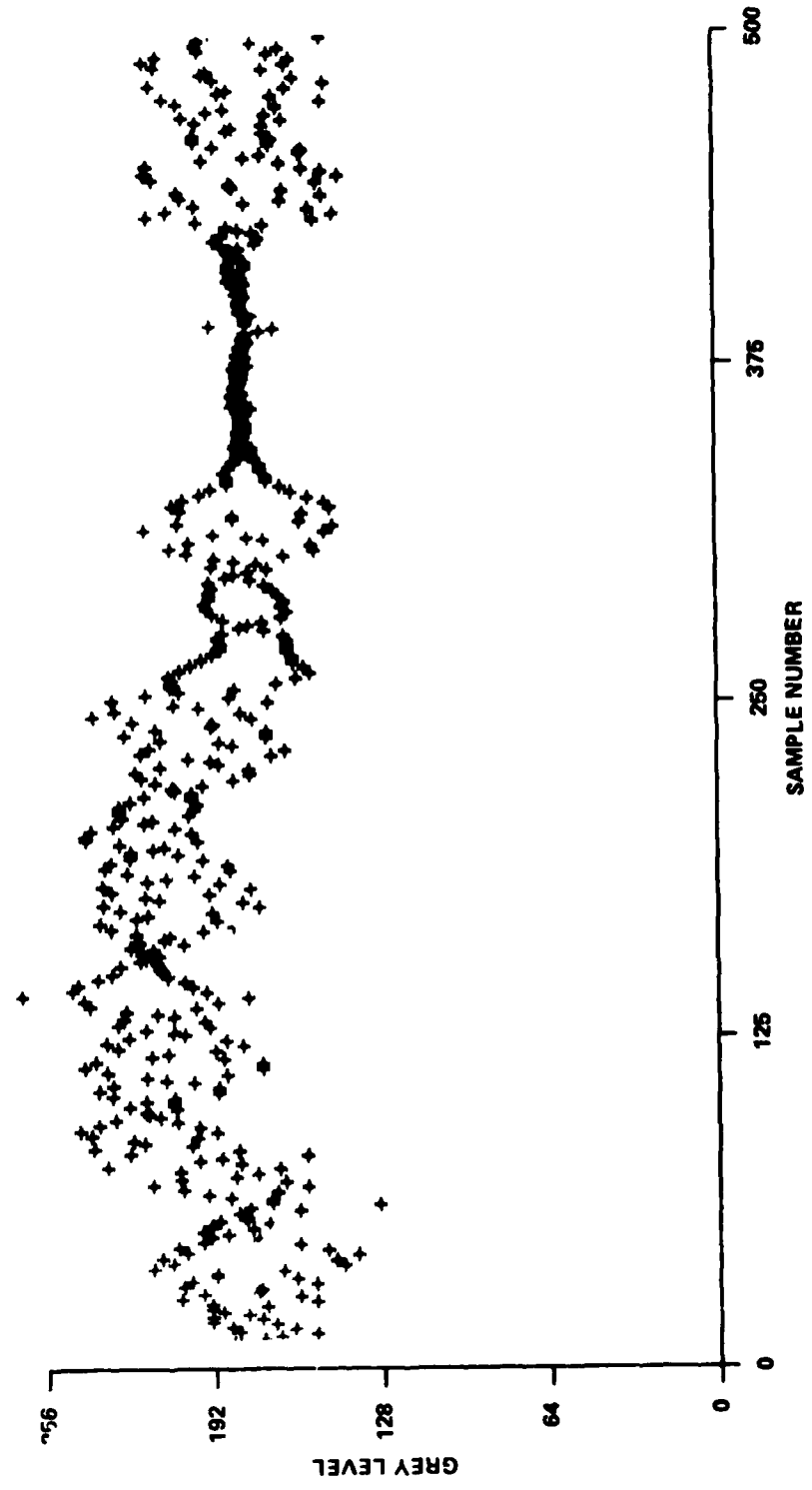


Figure 3. Grey level profile across the center of the initial image from left to right.

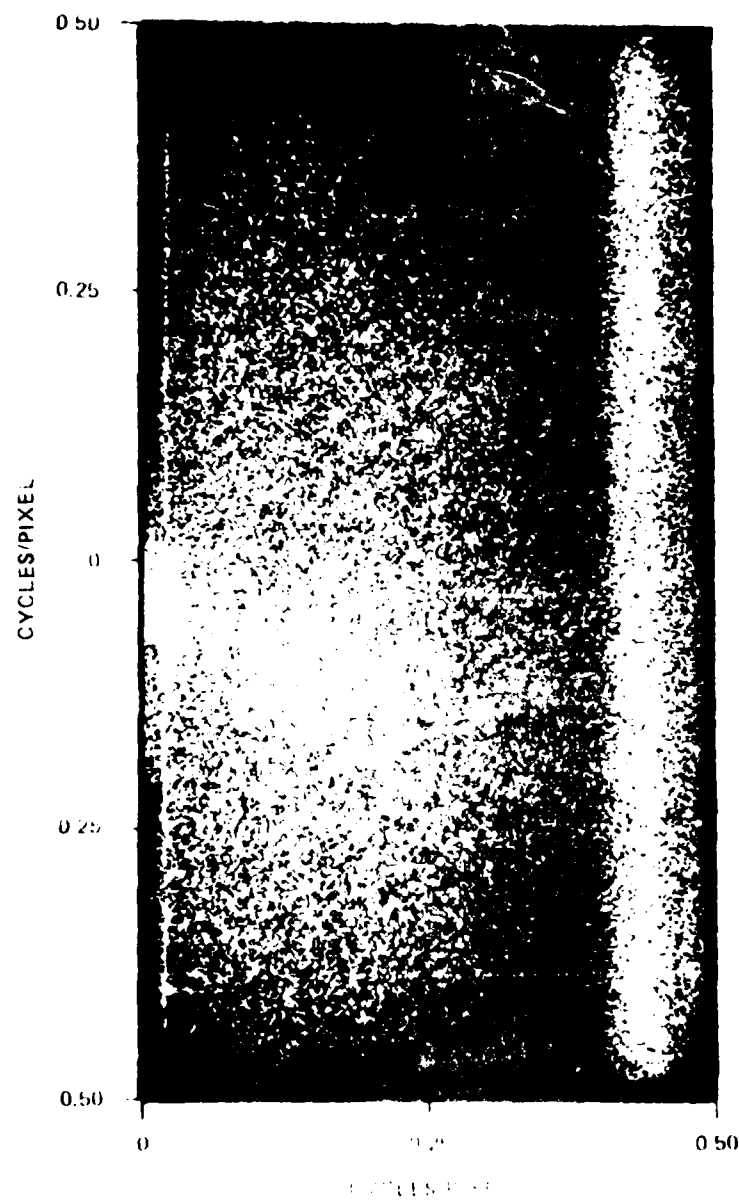


Fig. 1. 2D power spectrum

of the image with no filtering.

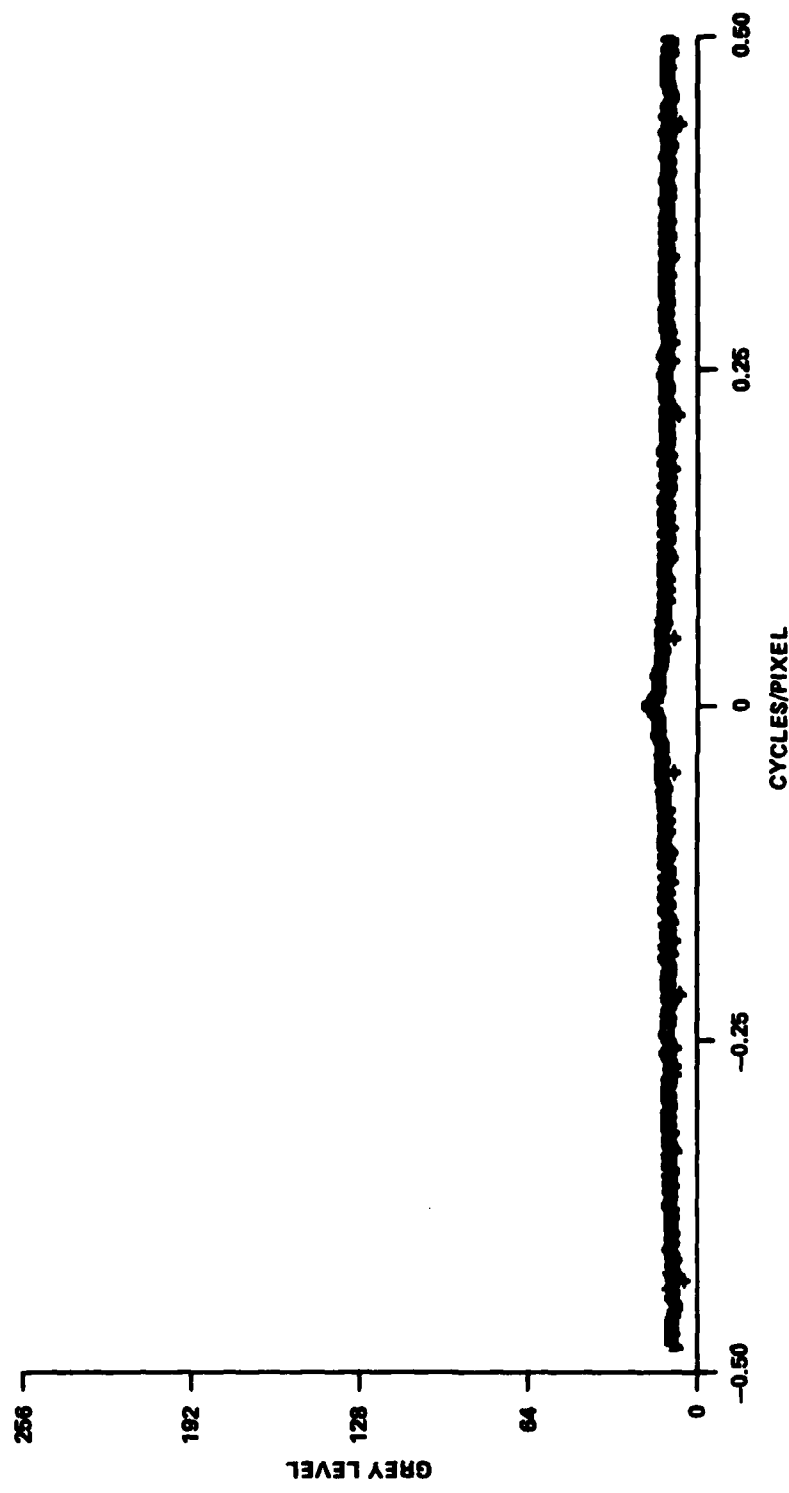


Figure 5. Profile of the transformed, unfiltered image along the vertical axis at 0 cycles/pixel on the horizontal axis.

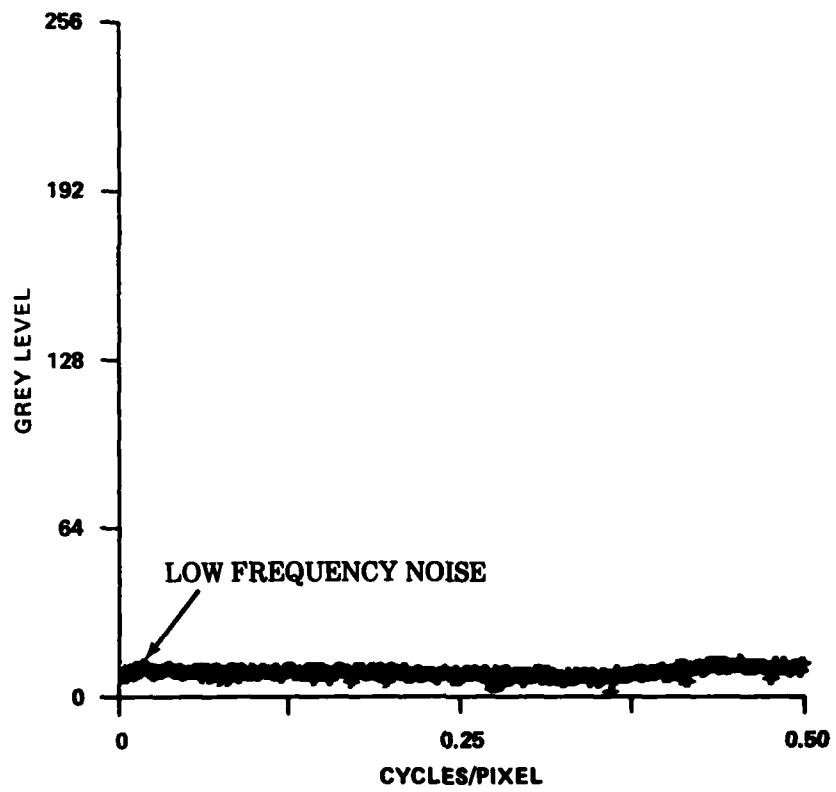


Figure 6. Profile of the transformed, unfiltered image along the horizontal axis at .5 cycles/pixel on the vertical axis.

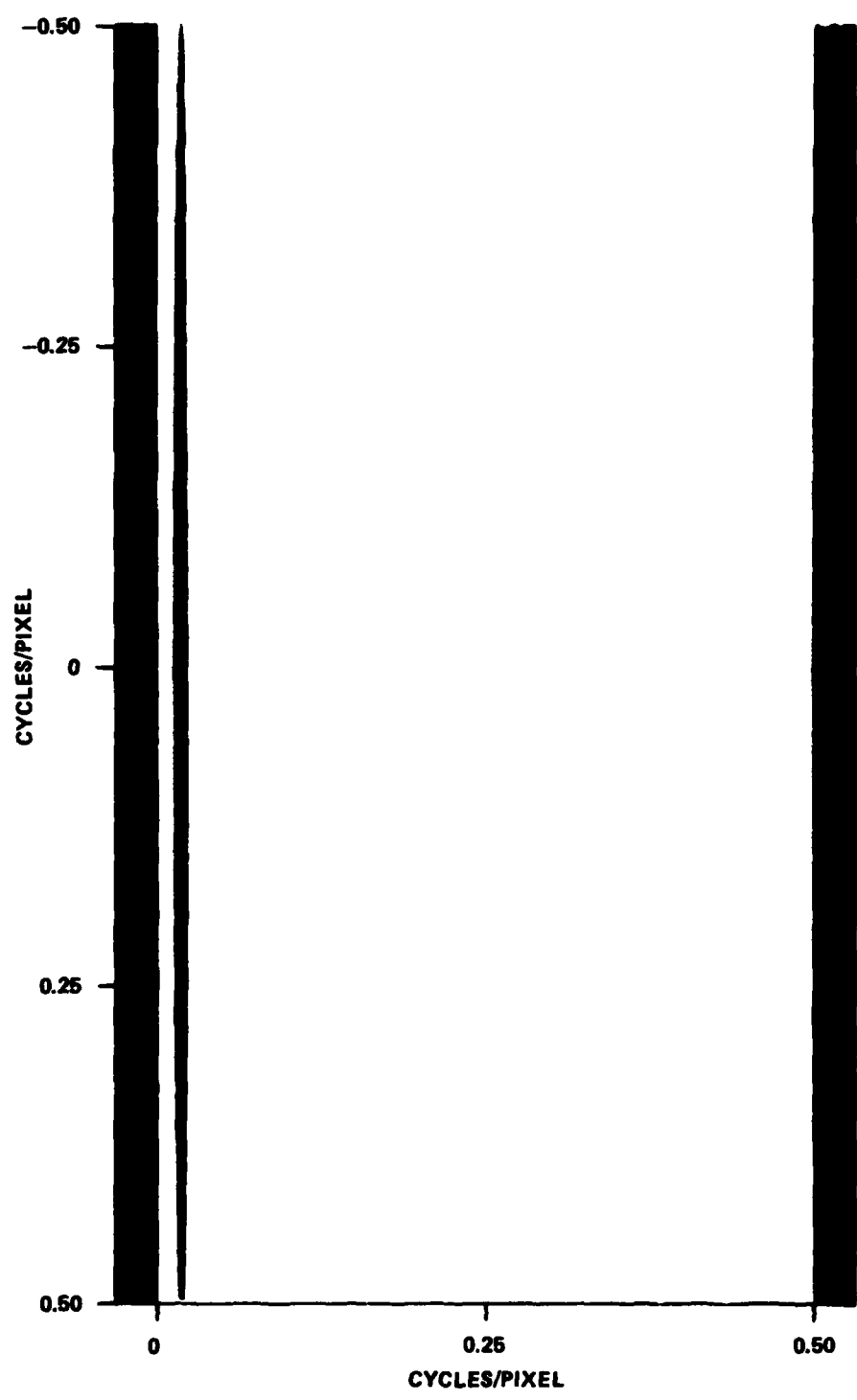


Figure 7. Top view of the inverse, Gaussian filter:
FILTER 1.

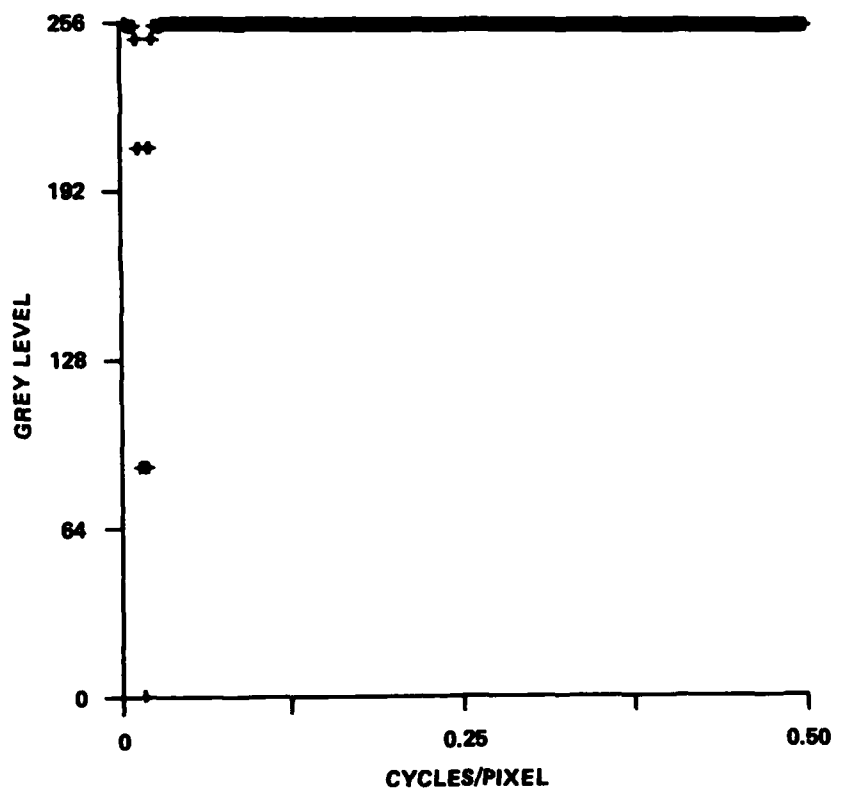


Figure 8. Profile of the inverse, Gaussian filter:
FILTER 1.



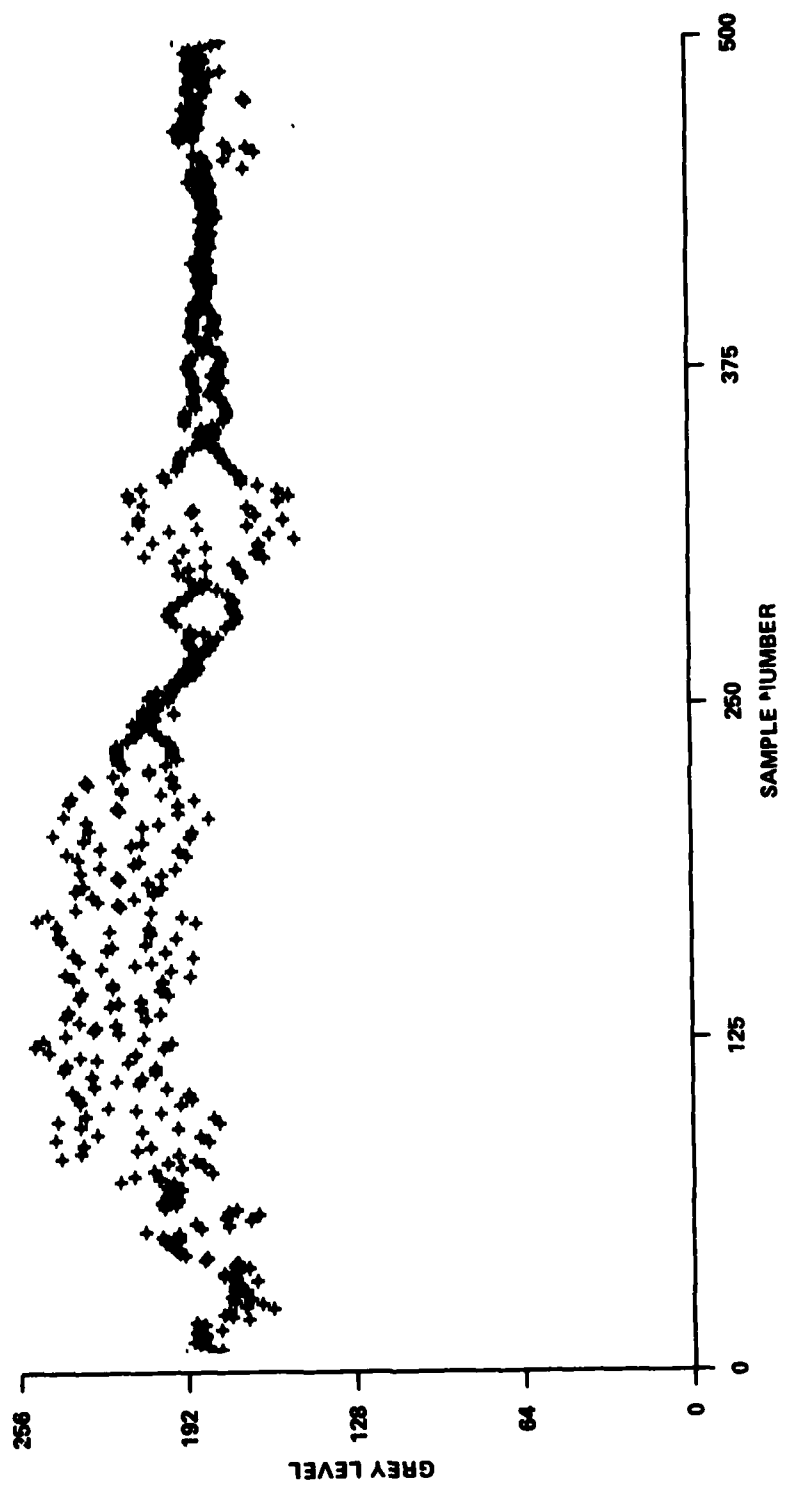


Figure 10. Profile of grey levels across the center of the image in figure 9.

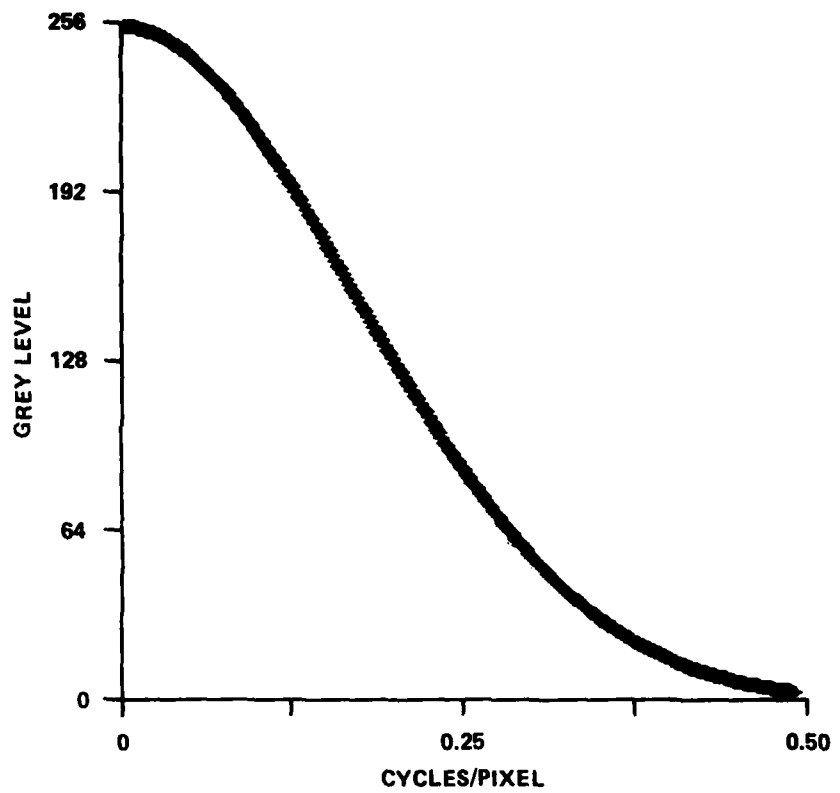


Figure 11. Profile of the low-pass Gaussian filter:
FILTER 2.

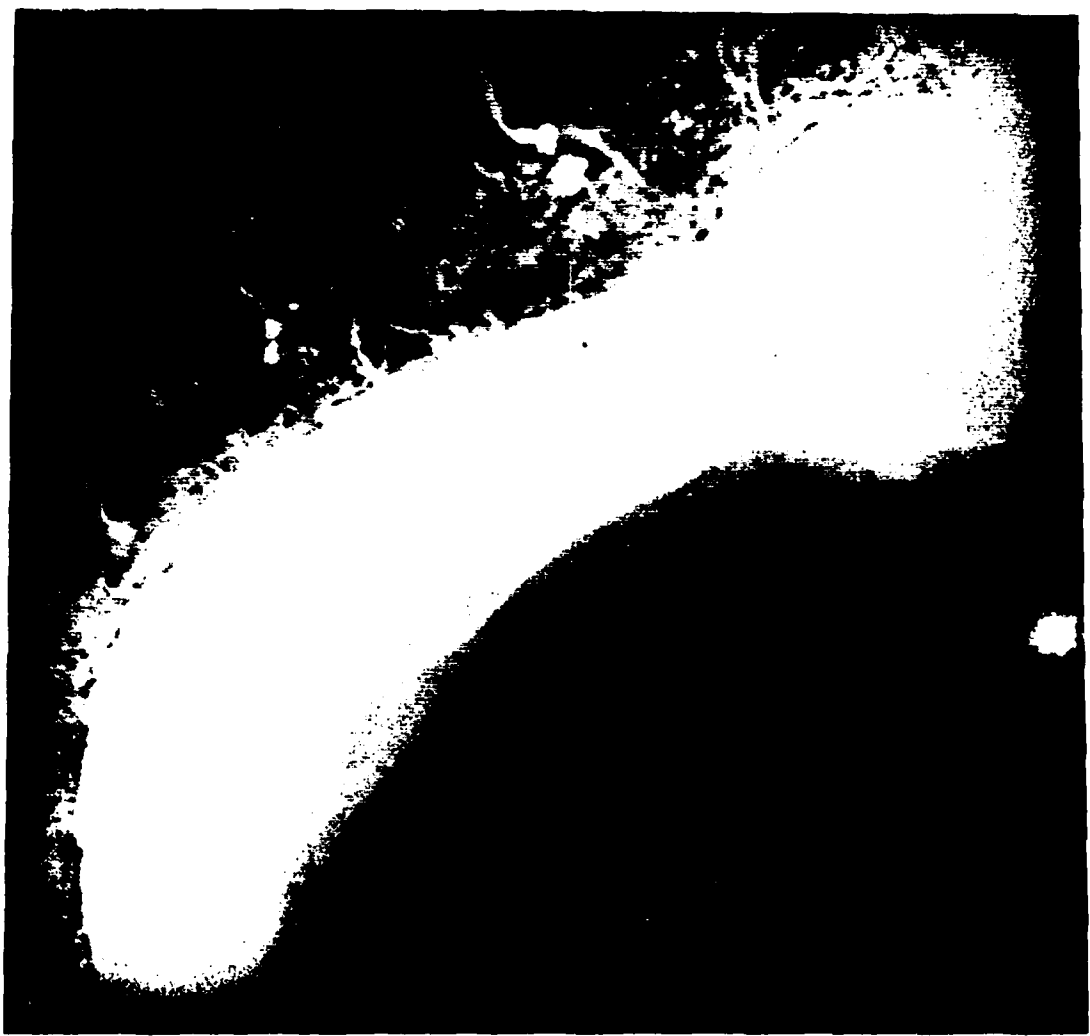


Figure 17. LFTD trace after applying a filter.

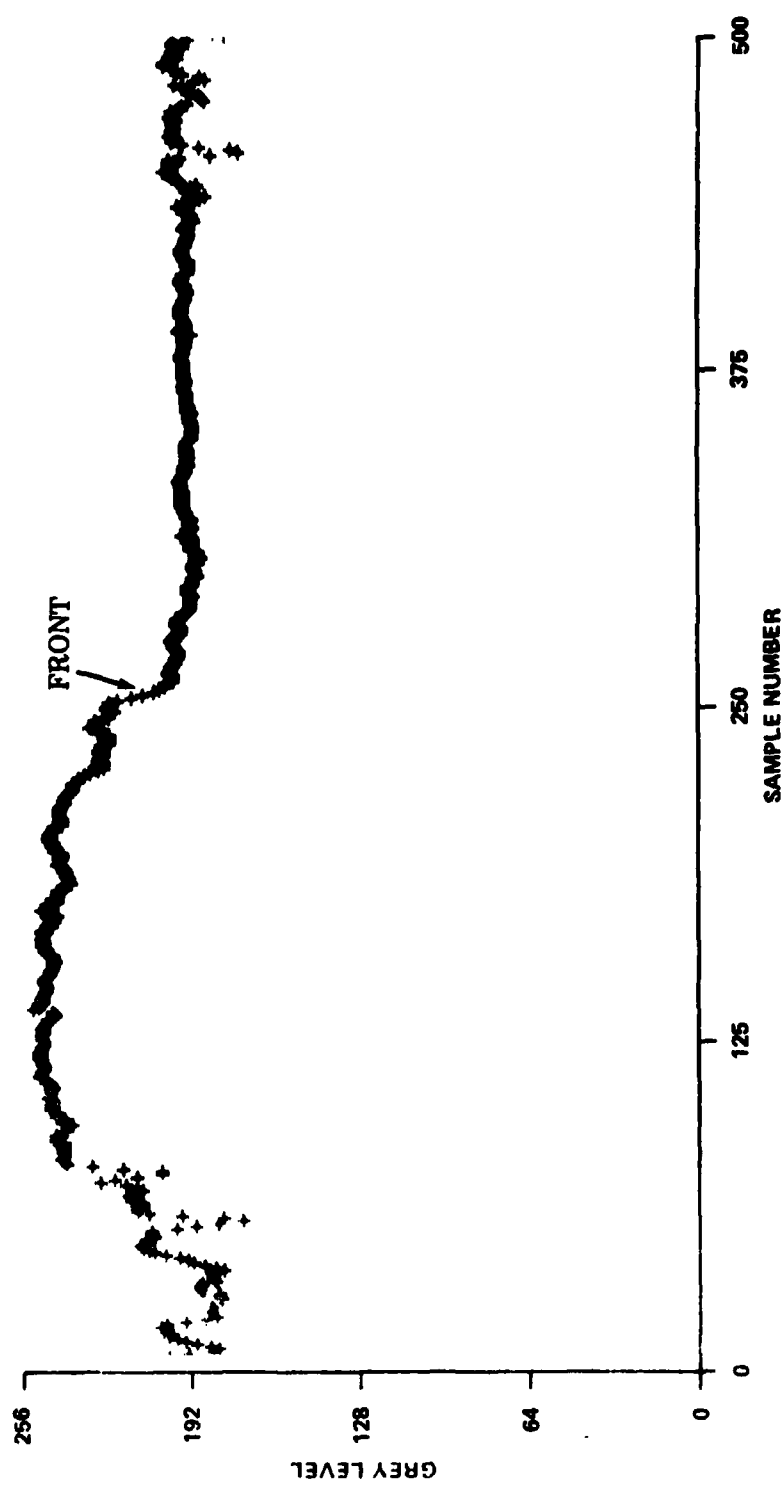


Figure 13. Profile of grey levels across the center of the image in figure 12.



Figure 1. A convolved image.

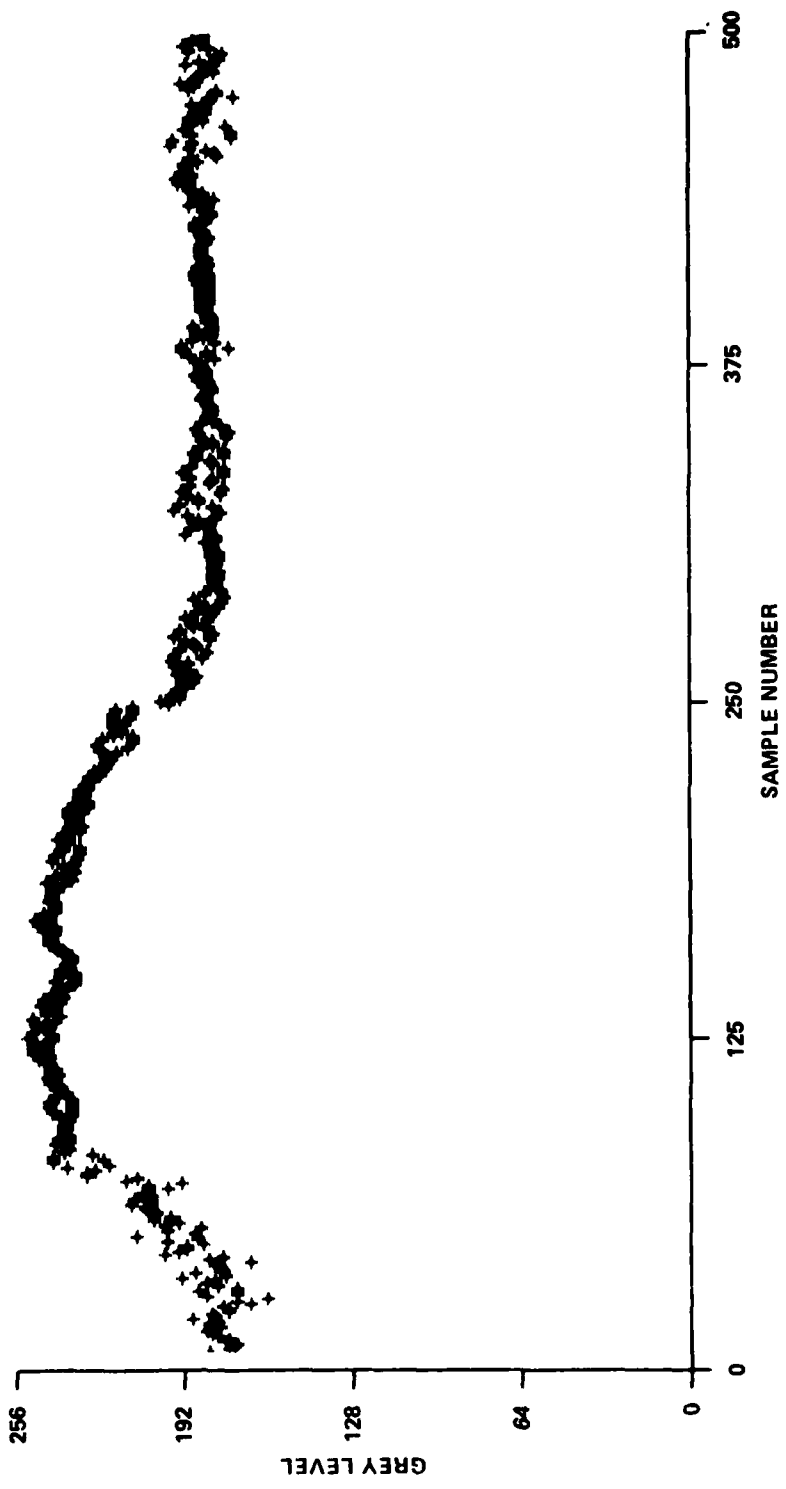


Figure 15. Profile of grey levels across the center of the image in figure 14.

DISTRIBUTION LIST

| <u>ACTIVITY</u> | <u>TOTAL NO. OF COPIES</u> |
|--------------------------|--------------------------------|
| CNO (OP 952, 952D1) | 2 |
| COMNAVOCEANCOM | 1 |
| FLENUMOCEANCEN (GTRL) | 1 |
| NORDA | 1 |
| NOSC | 1 |
| NRL | 1 |
| NUSC (22, 3343, Library) | 3 |
| JPL | 1 |
| ONR-Boston | 1 |
| GSO/URI | 1 |
| DO/TAMU | 1 |
| DO/UW | 1 |
| SIO | 1 |
| WHOI | 1 |
| DTIC | 12 |

DA
FILM